Lignite and Biomass Waste Hydrothermal Liquefaction Crude Upgrading by Hydrotreatment

N. Batalha, R. Checa, C. Lorentz, P. Afanasiev, K. Stanczyk, K. Kapusta, D. Laurenti, C. Geantet

▶ **To cite this version:**

N. Batalha, R. Checa, C. Lorentz, P. Afanasiev, K. Stanczyk, et al.. Lignite and Biomass Waste Hydrothermal Liquefaction Crude Upgrading by Hydrotreatment. Energy & Fuels, 2023, 10.1021/acs.energyfuels.3c01550 . hal-04170031

HAL Id: hal-04170031
https://hal.science/hal-04170031v1

Submitted on 24 Nov 2023

HAL is a multi-disciplinary open access archive for the deposit and dissemination of scientific research documents, whether they are published or not. The documents may come from teaching and research institutions in France or abroad, or from public or private research centers.

L'archive ouverte pluridisciplinaire **HAL**, est destinée au dépôt et à la diffusion de documents scientifiques de niveau recherche, publiés ou non, émanant des établissements d'enseignement et de recherche français ou étrangers, des laboratoires publics ou privés.

Hydrocarbon fuels from sequential hydrothermal liquefaction (HTL) of lignite and catalytic upgrading of crude oil

Nuno Batalha [a], Ruben Checa [a], Chantal Lorentz [a], Pavel Afanasiev [a], Krzysztof Stańczyk[b], Krzysztof Kapusta[b], Dorothée Laurenti [a], Christophe Geantet [a]*

[a] Université de Lyon, Institut de Recherches sur la Catalyse et l'Environnement de Lyon (IRCELYON), UMR5256 CNRS-UCB Lyon 1, 2 Avenue Albert Einstein, 69626, Villeurbanne Cedex, France

[b] Główny Instytut Górnictwa (Central Mining Institute), Plac Gwarków 1, 40-166 Katowice, Poland

* Corresponding Author: nuno.rocha-batalha@ircelyon.univ-lyon1.fr

ABSTRACT

Lignite from Belchatów in Poland was converted to hydrocarbon fuels, particularly in the kerosene and diesel range, through sequential hydrothermal liquefaction (HTL) and hydrotreatment (HDT) of the obtained crude oil. Different HDT temperatures were investigated (from 350°C up to 390°C). Despite the highly aromatic nature and high heteroatom content, the HTL lignite crude oil could undergo deep hydrodesulfurization (HDS = 99 %) and hydrodeoxygenation (HDO =98 %) in a single HDT treatment stage, yielding a liquid product rich in aliphatic and aromatic, particularly monoaromatic, hydrocarbons. The hydrotreatment and hydrogenating capacity of the lignite crude oil was linked to the low presence of refractory compounds in lignite and, consequently, lignite's crude oil, permitting the easy transformation of the crude oil into hydrocarbon fuel.

In addition to the crude oil, the HTL of lignite yielded a stream of char, which displayed a higher calorific value and lower heteroatom content than the original lignite feedstock, thus having a high potential for electricity production, the common use of lignite. Thus, introducing an HTL stage to extract crude oil before lignite use in electricity production could provide an alternative fuel source

used as a strategy to increase multiple countries' energetic independence before the transition to renewable fuels.

Keywords: Lignite; hydrotreatment; Crude oil; liquid fuels; coal valorization

1. INTRODUCTION

The Russian invasion of Ukraine in February 2022 has redistributed the energetic policy in Europe (and in the world) and deeply impacted the food and energetic markets and climate issues [1]. For instance, the European Union (E.U.) is the first market for diesel fuel and must import 20% of its consumption. Half of this imported diesel was coming from Russia. Despite E.U. policy attempts to eliminate fossil resources, with a new target of 45% of renewables in 2030, energetic transition and evolution of energetic policies are challenging to manage, and a portfolio of options must be investigated. Biofuels and biodiesel are slowly increasing their production. However, these are only expected to cover 4.6% of transport fuel demand in 2024[2]. Therefore, there might be a need for a local diesel resource in the E.U. before vehicles electrification and green fuels are fully implemented.

Despite its relatively low heat content, almost 80% of lignite is used for electricity generation[3]. Even if its production has strongly decreased since the 90's in Europe, the inland consumption of brown coal by E.U. member states was estimated, in 2021, at 300 Mt [4]. An alternative pathway to valorize lignite, pure or mixed with waste biomass, is hydrothermal liquefaction. In the absence of oxygen, subcritical or supercritical water as a reaction medium converts organic matter, independently of the origin, into a liquid of high heating value (HHV). In early works, Deshpande et al., Kershaw et al., and Hu et al. extracted brown coals or Dayan lignites, respectively, with sub and supercritical water and claimed that the extraction residue would be a good feedstock for combustion or gazification[5–7]. These studies led to the establishment of the hydrothermal dewatering (HTD) process, a pretreatment (developed at pilot scale) of lignite with no particular address regarding the crude oil formed [8]. This was only tackled more recently by Hartman et al., which investigated the HTL of selected coal feedstocks providing a high liquid yield (21%) and concluded that high-value petroleum-like products could be obtained [9]. Liu et al. used HTL as a pretreatment before pyrolysis of Xiaolongtan lignite and suggested three reaction steps discussed hereafter[10]. Like HTL of biomass, numerous reactions occurring during HTL are favorable for deoxygenation and monomer formation, even if condensation reactions may co-occur. Due to the complexity of the HTL process, the optimization of operating conditions, i.e., the impact of lignite nature and the understanding of the formation of the product, have yet to be deeply investigated. Recently, Li et al. attempted to optimize HTL process parameters for the transformation of demineralized and pretreated lignite, observing

these can impact the liquid yield and composition[11]. They also suggested that HTL promotes the transfer from polycyclic aromatic hydrocarbons to monocyclic aromatic hydrocarbons. All these studies indicate that HTL of lignite can potentially provide some fuel. However, no one attempted to upgrade lignite HTL oil like it was done with the HTL biocrudes of biomass or wastes.

In the present work, we investigated the HTL conversion of a Polish lignite and the catalytic upgrading of the HTL lignite oil obtained. A detailed study of the upgrading operating conditions and their impact on the nature of the products was performed. After upgrading, a diesel fraction was obtained, showing that a preliminary HTL stage can provide a fraction of a diesel source and increase the HHV of the fraction used for electricity generation.

2. EXPERIMENTAL

2.1. Hydrothermal liquefaction of lignite

Lignite from the coal mine of Bełchatów in Poland was used as feedstock. The physicochemical characteristics of the feedstock are presented in Table 1. The HTL experiments were conducted in a batch type 1000 ml stainless steel autoclave reactor (Autoclave Engineers, USA), equipped with a magnetically coupled mechanical stirrer. In each of the HTL experiments, 600 g of 10 wt% of lignite in water solution was used. After loading the reactor, the residual air was removed by nitrogen purging and vacuuming four times. Subsequently, the vessel was pressurized with N_2 (~2 bar) and then heated to 360 °C (reaction temperature) with a constant heating rate 10 ^{o}C/min and maintained at this temperature for 30 min (HTL reaction time). The pressure in the reactor vessel was self-generated.

After completion of the reaction, the autoclave was cooled to ambient temperature, and the gas samples were taken for analysis by micro-GC SRA instruments equipped with the following three modules: MolSieve 5 Å with backflush, PoraPLOT U, and Plot Al_2O_3/KCl. The HTL products mixture (crude oil, aqueous phase, and char) were then recovered from the reaction vessel. The separation of the products mixture obtained after the HTL processes was performed using a vacuum filtration technique. The post-reaction mixture was filtered on glass microfiber filters. The aqueous phase obtained was separated from the char. The reactor vessel and the char were washed with acetone,

and the solid fraction and the liquid organic fraction (crude oil) solution in acetone were separated by vacuum filtration. Next, the solid fraction was dried to constant weight in the laboratory drying oven at 105 °C. The filtered crude oil solution was concentrated using a rotary vacuum evaporator. The scheme of the process is presented in Figure S1.

Table 1. Physicochemical properties of lignite feedstock.

Proximate Analysis	Moisture $_{total}$ (wt.%)	50.59
	Organic matter (wt.% dry)[a]	72.48
	Volatiles (wt.% dry)[b]	41.99
	Ash (wt.% dry)	25.94
Ultimate analysis	C (wt.% dry)	50.53
	H (wt.% dry)	4.55
	N (wt.% dry)	0.56
	O (wt.% dry)	15.99
	S total (wt.% dry)	3.78
Calorific value$_{as\ received}$ (kJ/kg)		8 130
Calorific value$_{dry}$ (kJ/mol)		18 960

[a] Weight loss of dry sample upon combustion under air atmosphere (T = 575 °C).

[b] Weight loss of dry sample under inert atmosphere (T=950 °C)

The yields of the products were calculated based on dry, ash-free (daf) initial lignite using the following formulas:

$$Crude\ oil\ yield\ (wt.\%) = \frac{m_{crude}}{m_{lignite}} 100 \quad \text{Equation 1}$$

$$Char\ yield\ (wt.\%) = \frac{m_{char}}{m_{lignite}} 100 \quad \text{Equation 2}$$

$$Gas\ yield\ (wt.\%) = \frac{\sum^{i} Mw_i y_i PV}{RT m_{Lignite}} 100 \quad \text{Equation 3}$$

$$Aqueous\ phase\ solubles\ yield\ (wt.\%) = 100 - gas\ yield - char\ yield - crude\ oil\ yield \quad \text{Equation 4}$$

Where:

m_{crude}, m_{char}, and $m_{lignite}$ are the mass of recovered crude oil, recovered char, and initial lignite feedstock on a dry, ash-free (daf) basis;

Mw_i and y_i are the molecular weight and gas composition of compound i, respectively.

P is the residual reactor pressure at room temperature

V is the reactor volume occupied by gas (400 mL)
R, is the ideal gas constant
T, is the room temperature

2.2. Hydrotreatment of lignite crude oil

The hydrotreatment of the crude oil obtained from the hydrothermal liquefaction of lignite was performed under batch conditions using a 300 mL reactor from Parr (Model 4566). The hydrothermal conversion of 3 g of crude oil was performed in the presence of 25 g of n-heptane (solvent) and 1 g of sulfided $NiMo/Al_2O_3$ catalyst (See main properties in Table S1). Heptane was considered inert during the reaction and is used to provide enough volume inside the reactor to enable continuous stirring (≈ 700 rpm) and, consequently, facilitate the contact between HTL oil, hydrogen, and catalyst. Before reaction, the catalyst was activated through sulfidation carried at 400 °C for 3 h, under a continuous flow (4 L/h) of H_2S (15%) in H_2. After being sulfided, the catalyst is kept under an inert atmosphere (N_2) until being transferred into the reactor.

At room temperature and after flushing with H_2, the reactor was pressurized with 10 bar of H_2 to prevent catalyst deactivation during heating. After, the reactor was heated up to the reaction temperature, i.e., 350 °C, 375 °C, or 390 °C . Once the reaction temperature is attained (20 min), an additional pressure of 50 bar of H_2 was introduced into the reactor, reaching a reaction pressure of ≈ 100 bar. After the second H_2 introduction in the reactor, the crude oil hydrotreatment was performed for 1 h or 3 h leading to a pseudo-WHSV (Equation 5) of 3 h^{-1} and 1 h^{-1}, respectively. Additionally, a test where the reaction was stopped after introducing the 50 bar of H_2 was also performed, denominated t = 0 h, as a reference.

$$(Pseudo - WHSV(h^{-1}) = \frac{m_{oil}}{m_{cat} t_{reaction}} \qquad \text{Equation 5}$$

Where:

m_{oil} and m_{cat} are the mass of crude oil and catalyst, respectively,

$t_{reaction}$ is the reaction time.

After the reaction, the reactor was cooled to room temperature, and the residual gas was collected in a gas bag and analyzed with a micro-GC (SRA instruments) equipped with three modules: Molsieve 5Å (H2, CO, CH4), Hayesep A (CO2, C2 hydrocarbons), PLOT Al2O3/KCl (C3-C4 hydrocarbons).

The liquid and spent catalyst were separated through filtration, and the heptane in the liquid was evaporated, using a rotovapor apparatus, for 2 h at a pressure of 30 mBar and temperature of 40°C. The liquid remaining after evaporation was considered to be the liquid product from hydrotreatment. Elemental analysis was used to determine the coke deposited in the catalyst, i.e., coke equivalent to carbon in the spent catalyst.

The yields of the products obtained from the HDT reaction, i.e., liquid, solid, gas, H_2O, and H_2S were calculated through the following equations:

$$Liquid\ yield\ (wt.\%) = \frac{m_{liquid}}{m_{crude\ oil}} 100 \quad \text{Equation 6}$$

$$solid\ yield\ (wt.\%) = \frac{m_{solid}}{m_{crude\ oil}} 100 \quad \text{Equation 7}$$

$$Gas\ yield\ (wt.\%) = \frac{\sum^{i} Mw_i y_i PV}{RT m_{crude\ oil}} 100 \quad \text{Equation 8}$$

$$H_2O\ (wt.\%) = (O_{crude\ oil} - Gas\ yield\left(\frac{\%CO}{28} + 2\frac{\%CO_2}{44}\right)16 - Liquid\ yield.O_{liquid})\frac{18}{16} \quad \text{Equation 9}$$

$$H_2S\ (wt.\%) = (S_{crude\ oil} - Liquid\ yield.S_{liquid})\frac{34}{32} \quad \text{Equation 10}$$

Where:

$m_{crude\ oil}$, m_{solid}, and m_{liquid} are, respectively, the mass of crude oil to be hydrotreated, the excess of mass found in the catalyst after reaction ($m_{spent\ catalyst}$-$m_{fresh\ catalyst}$), and the mass liquid obtained after evaporation of n-heptane;

Mw_i and y_i are the molecular weight and gas composition of compound i, respectively.

P is the residual reactor pressure at room temperature

V is the reactor volume occupied by gas (≈ 263 mL)

R, is the ideal gas constant

T, is the room temperature

O, is the weight fraction of oxygen in the crude oil ($O_{crude\ oil}$) and liquid (O_{liquid}) determined by elemental analysis.

%CO and $\%CO_2$, are the weight fraction of CO and CO_2, respectively, in the gas

S, is the weight fraction of Sulfur in the crude oil ($S_{crude\ oil}$) and liquid (S_{liquid}).

2.3. Characterization methods

Elemental compositions (CHNS-O) of lignite, crude oil, hydrotreatment liquid, and spent catalyst were analyzed on a Thermo Scientific FLASH 2000 Organic Elemental Analyzer (accuracy of ± 0.1 wt%). Additionally, the S composition of the crude oil and hydrotreatment liquid samples were also quantified using ANTEK 9000NS apparatus, which is more precise (from few ppm until percent levels) and accurate. Prior to analysis, the samples were diluted in THF (≈ 5 wt.%).

The boiling point of the sulfur-containing compounds in the crude oil was estimated by using a Agilent 7890A GC coupled with an FPD+ detector and fitted with a CP-SimDist GC column (10 m × 0.53mm × 2.65 µm).

The molecular weight distribution of the compounds in the lignite crude oil and the hydrotreatment liquid was obtained by size exclusion chromatography (SEC) performed using an Agilent 1200 series HPLC equipped with two PLgel Columns (50 and 500 Å), a refractive index detector (RID), and a diode array detector (DAD). The analysis was carried out at 35 °C using tetrahydrofuran (THF – 1 mL/min) as the eluent. Before analysis, the samples were diluted to a concentration of ≈1 wt.% in THF and filtered (0.45 µm). A mixture composed of hydrocarbons (Mw from 86 to 1000 g/mol) was used as standard to convert elution time into molecular weight (hydrocarbons equivalent) leading to an average Mw_{HC} data.

The ^{13}C-NMR analysis of the liquid samples was performed in a Bruker AVANCE 400 MHZ spectrometer and analyzed using the software TopSpin 3.0. The measurements were performed at room temperature with an accumulation of 4700 scans for approximately 15 h. The samples (≈100 mg) were diluted with deuterated chloroform ($CDCl_3$) (0.6 mL). Table S2 includes the chemical shifts attributed to each functional group.

Comprehensive GC×GC-TOF MS and GC×GC-FID were used to identify and quantify the compounds in the lignite crude oil and HDT liquid. The GC×GC/TOF system was equipped with a cryogenic modulator from Zoex Corporation (USA) and a BenchTOF 2 TI spectrometer from Sepsolve. The chromatograph

and TOF parameters are described in Tables S3 and S4. The GC×GC/FID was equipped with a switch valve modulator (Agilent G3486A CFT modulator), and modulation parameters were optimized according to ref [12]. The parameters used for product separation are described in Table S3. The quantification of the compounds detected by GC×GC-FID was performed using the relative responsive factor method (RRF)[13] with cyclohexanol as the reference. The data obtained from comprehensive GCxGC-FID was also used to provide the distillation curve of the HDT liquid products by using a mixture of n-alkanes (C_7 to C_{40}) as a reference.

3. RESULTS AND DISCUSSION

3.1. Hydrothermal liquefaction of lignite

3.1.1. Crude oil

While the primary target product for liquid fuel production is crude oil, only 12.3 wt.%daf of lignite was transformed into this product with char (48.8 wt.%daf), gas (23wt.% daf), and aqueous phase organics (15.9 wt.%daf) representing the main fractions. Liu et al. [21] studied the optimal conditions for maximizing crude oil yield from lignite HTL and found that short residence times, i.e., ~5 min, and high temperatures, i.e., ~400 °C, are necessary. In this study[21], the authors found a maximum crude yield of 34 wt.%. Hence, the high residence time (30 min) and low temperature (360 °C) presently used can explain the low crude oil yield. Another important parameter known to affect the yield and quality of crude oil in HTL is the amount of ash [25–29]. On biogenic feedstocks, such as algae, high ash contents have been reported to decrease the yield and quality of the crude product [25–27]. Although no reference applied to the conversion of lignite under HTL conditions was found, a direct analogy with biomass feedstocks suggests that high-ash in lignite might have a similar effect. Thus, a high concentration of ash found in lignite (25.94 wt.%) could also be responsible for the low crude oil yield (12.3 wt.%). Indeed, Liu et al. [21] used lignite with 7.14 wt.% of ash. It should be mentioned that Oner et al. demonstrated that ash positively enhances the crude oil product in lignite liquefaction under organic solvents, like tetraline, and under H_2 pressure [30]. However, the positive effects were attributed to the capacity of certain elements in ash to promote hydrogenation by H_2 or hydrogen transfer from the

219 solvent, a reaction not likely to occur under HTL conditions. While ash is bound to affect lignite HTL
220 conversion, the chemical composition of lignite and lignite's ash is substantially different from that of
221 biomass feedstocks like algae. Thus, further studies, out of the scope of this work, should be
222 performed to infer the impact of this component.

223 When compared to the lignite feedstock, the crude oil stream contains a higher concentration of
224 carbon (77.7 wt.% vs. 50.5 wt.%dry) and hydrogen (8.9 wt.% vs.4.6 wt.%dry) (Tables 1 and 2).
225 Additionally, the crude oil displayed a lower concentration of oxygen (10.8 wt.% vs. 16.0 wt.%dry) and
226 sulfur (2.4 wt.% vs. 3.78 wt.%dry) than the parent lignite sample. However, it is essential to mention
227 that the sulfur content in crude oil is still well above the specifications for liquid hydrocarbon fuels,
228 e.g., diesel specification < 10 ppm. Thus, significant desulfurization must take place during upgrading.
229 In the case of nitrogen, no specification states a maximum N concentration in hydrocarbon fossil
230 fuels[31]. Still, nitrogen compounds impact other regulated properties, such as gum content, storage
231 stability, and thermal stability [33]. However, synthetic aviation fuels (SAF) have a nitrogen
232 concentration inferior to 2 ppm[32]. It is worth mentioning that there is still no regulation concerning
233 HTL-derived fuels.

234 The functional group's composition, determined by ^{13}C NMR, of the crude oil is shown in Table 2. The
235 crude oil is mainly composed of aliphatic (53.6%) and aromatic (40.3%) carbon. Among the aromatic
236 carbon, 24.0% corresponded to C-H bonds, 9.6% to C-C bonds, and 6.8% to C-O bonds (chemical shift
237 and NMR Spectrum in Table S2 and Figure S2, respectively). Alkyl groups or polyaromatics compounds
238 in crude oil can explain the occurrence of C-C bonds in aromatic fraction. Additionally, the high
239 incidence of aromatic C-O and carbonyl C=O , compared to the methoxy, aliphatic, carboxylic acid, and
240 esters, indicates that phenolic compounds and ketones represent a significant portion of the crude oil
241 oxygen. Indeed, the crude oil composition analysis by comprehensive GC×GC-TOFMS (Figure 1)
242 showed the presence of ketones, furans, phenols, and naphthols. A small amount of mono-aromatic
243 and di-aromatic hydrocarbons and non-aromatic cyclic hydrocarbons, possibly derived from

biomarkers typically present in lignites[34], were also found. The quantification performed by GCxGC-FID is shown in Table 3. Only 16.7 wt.% of the crude oil sample was detectable by GCxGC-FID analysis. The non-detected compounds were too heavy to be analyzed by gas chromatography. Indeed, Liu et al. analyzed the heteroatom-containing compounds obtained from the ethanolysis of lignite via Fourier transform ion cyclotron resonance mass spectroscopy (FTICR-MS), observing a significant number of oxygenated compounds with up to 6 aromatic rings with the particular occurrence of oxygenated molecules with carbon number between 17 and 26 carbons and two oxygen atoms, like organic acids and diols[35]. In the same study, authors characterized the sulfur-containing compounds, mostly ranging above C_{20} and associated in the same molecule with another S or several O atoms. [35]. The relatively large carbon number of the sulfur-containing compounds in crude oil can explain the few S compounds detected in the products by comprehensive GCxGC-TOFMS (Figure 1). Indeed, the analysis of the sulfur content of the crude oil sample by GC-FPD^+ using a Simdis chromatography method equivalent to ASTM D2887 reveals that such molecules have a retention time higher than hexatriacontane (C_{36} - Bp = 497 °C) (Figure S3), which defines the upper detection limit of the GCxGC analysis. The same explanation can be given for the few nitrogen-containing compounds among the GC×GC detected compounds in the crude oil (Figure 1).

Table 2. Composition of crude oil obtained from the HTL of Bełchatów lignite

Composition		Carbon chemical composition (^{13}C NMR)[a]	
C (wt.%)	77.7± 0.1	$C_{Aliphatic}$	53.6
H (wt.)	8.9 ± 0.3	$C_{Methoxy}$ (-O-$CH_{3)}$	0.1
O (wt.%)	10.8 ± 1.0	$C_{Aliphatic-O}$ (-O-$(CH_2)_n$)	0.8
S (ppm)	2.4 ± 0.1	$C_{aromatic}$	40.3
N (ppm)	0.5 ± 0.1	$C_{Carboxylic/Amide}$	0.8
TAN (mg_{KOH}/g)	29.2 ± 0.2	$C_{Aldehyde/Ketone}$	4.4
HHV (MJ/kg)	31.8		

[a]Chemical shift range in Table S1 and NMR spectra in Figure S2

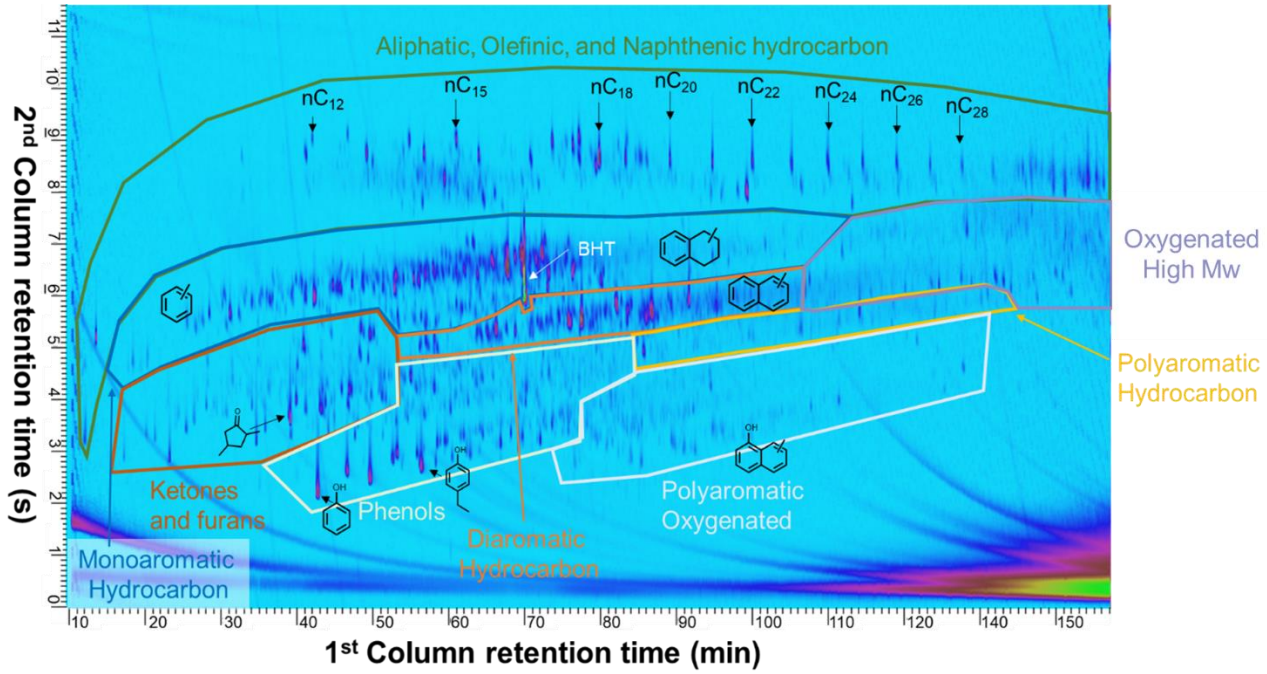

262

263 Figure 1. GCxGC-TOF MS chromatogram of the crude oil obtained from the HTL of lignite. BHT
264 (butylated hydroxytoluene) originates from THF solvent, where it serves as a stabilizer.

265

266 Table 3. Quantification of the lignite HTL oil compounds detected by GCxGC-FID using the relative
267 response factor method (supporting information). The chromatogram and the areas attributed to
268 each compound family are represented in Figure 1.

Compounds	Oil composition (wt.%)	Compounds	Oil composition (wt.%)
Aliphatic HC	1.6	Ketones and furans	0.6
Monoaromatic HC	1.6	Phenols	1.4
Diaromatic HC	1.6	Polyaromatic Oyxgenated	2.2
Polyaromatic HC	1.2	Aliphatic Oxygenated	6.5

269

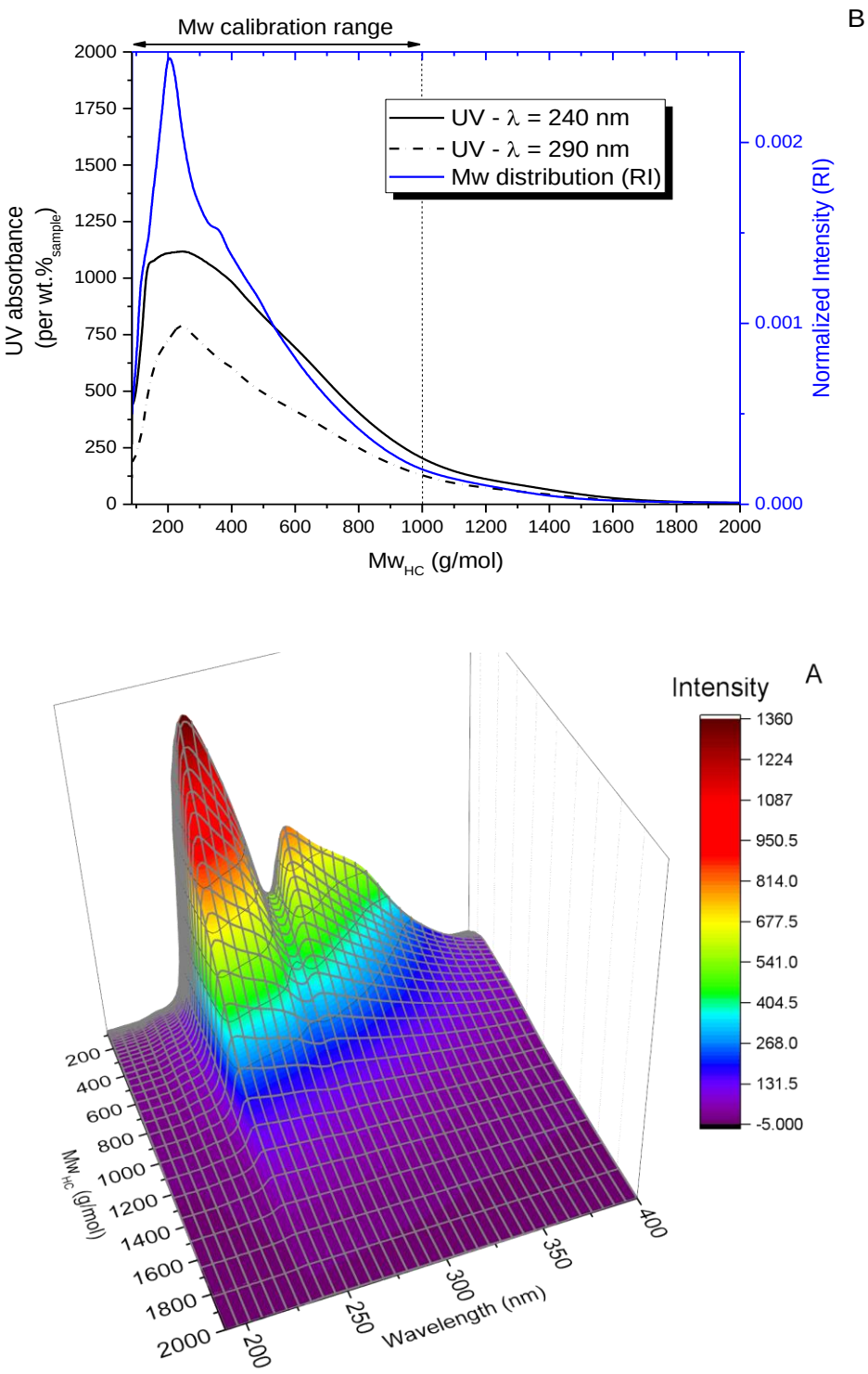

Figure 2. A) Compounds in the liquid product molecular weight (Mw_{HC}) distribution determined by refraction index (RI) (blue curve) and UV absorbance (λ = 240 nm and 290 nm) as a function of the compounds Mw. Average Mw = 297 g/mol. B) DAD spectrum ((λ = 190 - 400 nm) of crude oil as a function of molecular weight (Mw_{HC}).

277 A better insight into heavy molecules is given by SEC. The molecular weight distribution of the crude
278 oil components (Figure 2-A) reveals a large range of compounds, with a molecular weight of up to
279 ~1,800 g/mol in HC eq. and an average molecular weight of 297 g/mol in HC eq. The significant
280 presence of large Mw molecules, which are expected to have a high boiling point, agrees with the
281 small detection level observed in the GCxGC analysis. The evolution of the DAD spectra as a function
282 of molecular weight (Figure 2-B) reveals an intense absorption between 240 and 400 nm, reflecting
283 the high aromatic nature of the compounds in the crude oil. The presence of two absorption
284 maximums, 245 nm and 293, and a shoulder at 316 nm indicates that polyaromatic compounds are
285 abundant in the crude oil sample. Indeed, as exemplified in Figure S4, monoaromatic compounds like
286 benzene generate a DAD band at ~250 nm. In opposition, polyaromatic compounds with two or more
287 conjugated aromatic rings present a second absorption band at $\lambda > 290$ nm (Figures S5, S6, and S7). In
288 the particular case of naphthalene, a second sharp peak was observed at 290 nm, with identical
289 intensity to the peak centered at 250 nm (Figure S5), while in anthracene and pyrene, this band is
290 significantly broader, extending to significantly higher λ (Figures S6 and S7). Therefore, in the crude
291 oil (Figure 2-A), the wide absorption band at $250 > \lambda > 400$ nm indicates the presence of compounds
292 with at least 3 and 4 conjugated aromatic rings.

293 The comparison of the Mw distribution and the UV absorbance at λ=240 nm and 290 nm as a function
294 of the Mw reveals that both RI and UV curves have a maximum at Mw ~ 230 g/mol (Figure 2-A).
295 However, the UV spectra absorption distribution is shifted to higher Mw, evidencing heavier
296 molecules with high aromaticity presence.

297

298 ***3.1.2. Char, gas, and aqueous phase***

299 The hydrothermal liquefaction of lignite (soft Miocene lignite) obtained in the Bełchatów coal mine in
300 Poland led to four product streams, i.e., gas, char, crude oil, and an aqueous phase rich in organic
301 matter. Char was the most abundant among the product streams, representing 48.8 wt.% of the lignite

feedstock yield. Even though char and lignite are both solids, the former displayed a higher carbon content with lower oxygen, nitrogen, hydrogen, and sulfur (Table S4). Hence, char displayed O/C and H/C ratios of 0.1 and 0.4, respectively, while lignite O/C was 0.2 and H/C was 1.1. The different solid composition explains char's slightly higher heating value compared with the lignite feedstock, i.e., 22.6 MJ/kg_{Dry} vs. 19.0 MJ/kg_{Dry}, respectively. P. Liu and D. Zhang[14] studied the transformation of lignite under hydrothermal conditions, observing that, at T=260 °C, significant removals of oxygen and hydrogen occur. Similar observations were made by Z. Shi et al. [15], who, like P. Liu and D. Zhang, observed a significant reduction of carboxyl, carbonyl, and oxygenated aliphatic carbon in the solid after HTL treatment. These authors also observed a reduction of the aliphatic CH_2 and CH_3 groups after hydrothermal treatment, which justifies the decrease in the H/C ratio. The authors linked the elimination of oxygen and hydrogen from the lignite structure to the production of light gases, such as CO, CO_2, and light hydrocarbons[14,15]. Like O and H, the sulfur in char was significantly smaller than in the lignite feedstock, i.e., 1.1 wt.% vs. 3.78 wt.%, respectively, indicating only 14.2 % of sulfur remained in the solid phase after hydrothermal liquefaction. The significant extent of desulfurization is directly related to the nature of the sulfur compounds in lignite. As low-ranking coals, lignites contain more substantial amounts of sulfides and thiols than other types of coal[16], which are more easily transformed under hydrothermal conditions[17,18].

The lower impurities content, i.e., O, N, and S, and increased calorific value indicate that char is a higher quality coal than the original lignite. Indeed, the treatment of coal samples through hydrothermal liquefaction has been demonstrated to increase the quality of coal samples, both by eliminating impurities and improving hydrophobicity[11,15,19,20].

The composition of the gas stream formed during the hydrothermal liquefaction of lignite is shown in Table S5. CO_2 was the majority product in the gas phase, corresponding to 92.6 wt.% of all the produced gases. The high CO_2 selectivity in the gas products obtained from lignite HTL had already been reported previously[15,21], indicating that decarboxylation is one of the primary processes responsible for oxygen removal during the reaction. Indeed, CO only represented 1.4 wt.% of the

gases, suggesting decarbonylation is significantly less favored. H_2S represents the second most abundant compound in the gas stream, representing 3.4 wt.% of all gases. Furthermore, 19.4% of the sulfur in the lignite feedstock was transformed into H_2S. The significant formation of H_2S reflects the transformation of organic, i.e., thiol and sulfide, and inorganic sulfur, i.e., pyrite, compounds in lignite promoted by H radicals under hydrothermal conditions [17,18,22]. In addition to CO_2, CO, and H_2S, small amounts of light hydrocarbons and H_2 (Table S5) were also observed. Nonetheless, the amount of such compounds is not enough to justify alone the small H/C observed in the char, thus suggesting that light hydrocarbons and H_2 formation are not the main ones responsible for the elimination of hydrogen in the lignite as proposed by Z. Shi et al., and P. Liu and D. Zhang [14,15]. Instead, the transformation of lighter fractions of lignite into aqueous and crude organic compounds is more likely to cause the low H/C of char compared to lignite.

Finally, the organic matter solubilized in the aqueous reaction media, i.e., the aqueous phase, represented 15.9 wt.% of feedstock lignite. In hydrothermal liquefaction processes, the aqueous phase is typically composed of organic acids, e.g., acetic acid, oxygenated aromatics, aromatic, like phenols, nitrogenated compounds, and oxidized sulfur compounds[18,23,24], thus justifying this stream's acidic pH of 5.2.

3.2. Hydrotreatment of lignite HTL crude oil

The significant concentration of heteroatoms and polyaromatic compounds in the crude oil stream clearly demonstrates the necessity of further upgrading for the production of hydrocarbon fuels. Therefore, this section will focus on the hydrotreatment of the crude oil stream obtained from the hydrothermal liquefaction of lignite. The hydrotreatment of the lignite crude oil was performed at three different temperatures, i.e., 350 °C, 375 °C, and 390°C, and at two different reaction times, 1 h and 3 h. An additional residence time, where the reaction was stopped after the reaction temperature was attained ($t_{heating}$ = 20 min), designated t = 0 h, was also performed at each temperature. The crude

353 oil conversion occurring before t = 0 h are caused primarily by thermal processes. For each operating
354 condition, five product streams (Figure 3-A) were obtained, i.e., gas, liquid, solid, and H_2S and H_2O
355 estimated using equations 9 and 10.

356 ***3.2.1. Solid product***

357 The solid product, which was determined through the difference in the catalyst weight before and
358 after the reaction (equation 7), was found to decrease as a function of the reaction time. Indeed, for
359 the t = 0 h experiments, the solid fraction yield was ≈ 16.7 –19.6wt.%, while the solid yield decreased
360 to ≈ 9 – 12 wt.% for longer residence time. It should be mentioned that no solid matter other than the
361 spent catalyst was found in the reactor. Consequently, at least part of the solid product is represented
362 by heavy asphaltene-like products that can be converted under the reaction conditions but are not
363 soluble in heptane and stay with the catalyst after the reaction. Table S6 contains the carbon loading
364 of the spent catalyst after the reaction, showing that higher reaction time and temperatures lead to
365 lower carbon deposition on the catalyst's surface. Furthermore, at the temperature of 375 °C and 390
366 °C after 3 h, the carbon deposition on the spent catalyst was ≈ 5 wt.%, which is compatible with the
367 typical coke loadings observed in the early stages of operating HDT catalysts[36]. Hence, the crude oil
368 feedstock did not lead to enhanced deactivation by coke deposition of the sulfided catalyst, as
369 observed for HTL crude oils from other sources, like sewage sludge [37].

370 ***3.2.2. Gas product***

371 The yield and composition of the gas products are shown in Figure 3-B. In general, the yield of gas
372 increases with the reaction temperature and reaction time, achieving a maximum of 4.7 wt.% for the
373 reaction conditions of 390 °C and 3 h. Still, the yield of gas products like CO and CO_2, which result from
374 decarboxylation and decarbonylation reactions, was found to stay constant, between 0.4-0.6 wt.%
375 and 0.6 – 0.8 wt.%, respectively, after 1 h of reaction independently of the temperature (Figure 3-B).
376 The low yield of CO and CO_2 is attributed to the minor contribution of aliphatic C-O, methoxy, and acid
377 groups in the crude oil (Table 2). Indeed, the oxygen in the crude oil was primarily eliminated as H_2O,

whose yield is between 7.5 wt.% and 10.0 wt.%. Light hydrocarbons, like CH_4, C_2H_6 (C_2), C_3H_8 (C_3), and C_4H_{10} (C_4), were the main compounds responsible for the gas yield increase observed at higher temperature and reaction time (Figure 3-B). While the formation of light hydrocarbons can be explained by C-C bound cleavage caused by hydrogenolysis, which is favored at higher temperatures, heptane hydrogenolysis does not seem to contribute significantly to the gas products since the $\frac{C_3}{C_4}$ ratio is significantly higher than 1 (Figure 3-B). Instead, light hydrocarbons most likely result from the cleavage of larger molecules from the crude oil during the hydrotreatment reaction. However, it is worth mentioning that, after 3 h of reaction, the O content in the liquid product is quite low for the catalytic tests performed at 375 °C and 390 °C (Figure 4), and the contribution of light hydrocarbons to the gas yield is significantly higher at 390°C. Hence, the occurrence of C-C hydrogenolysis and its contribution to the gas yield cannot be discarded entirely.

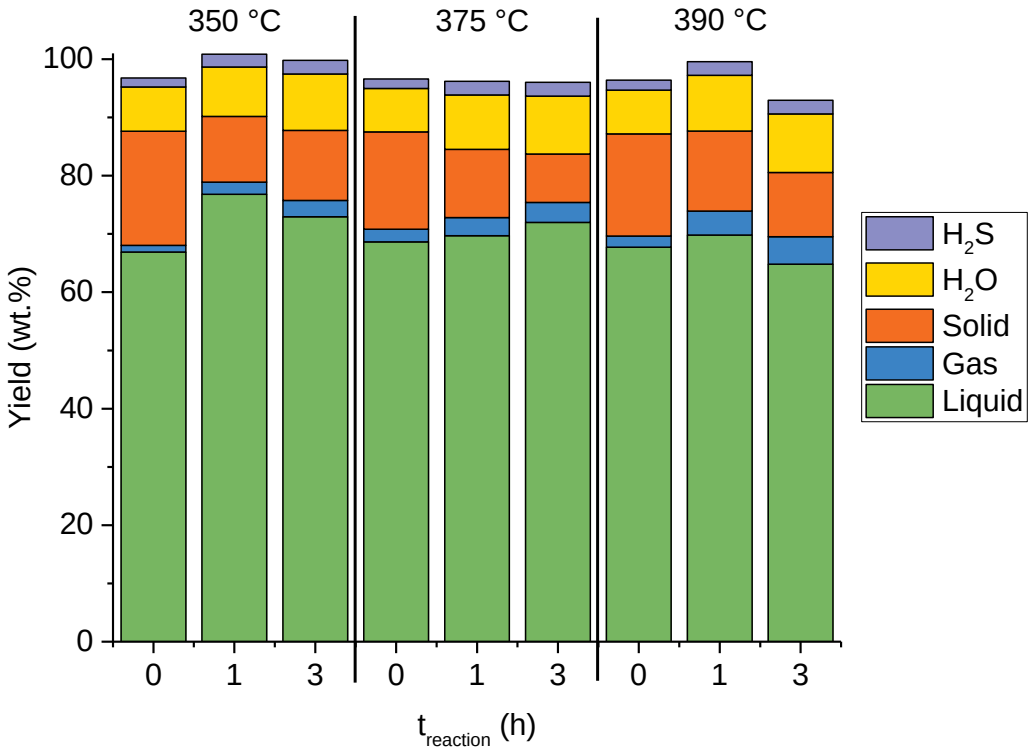

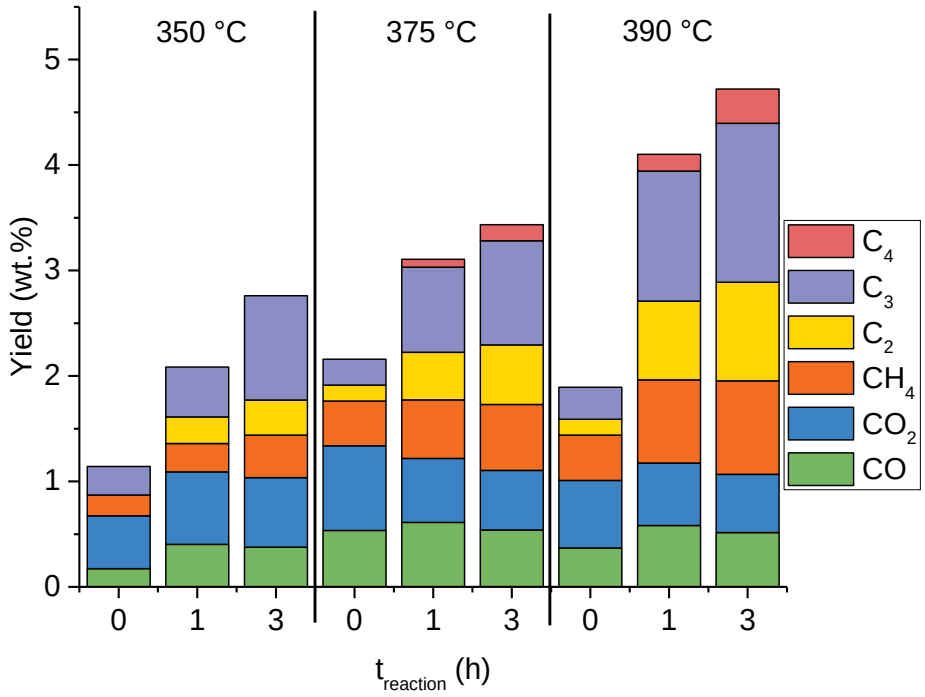

Figure 3. A) Product yields, determined according to equations 6 to 10, obtained from the HDT of the lignite HTL crude oil. B) Gas products yield as a function of reaction temperature and time, obtained from the HDT of the lignite HTL crude oil.

3.2.3. Liquid product

After upgrading, the liquid product yield varied between 65 wt.% and 77 wt.% depending on the reaction temperature and time (Figure 3-A). In all cases, the liquid yield was higher after 1 h of reaction as compared to $t_{reaction}$ = 0 h, which agrees with the hypothesis previously stated on the conversion of solid products existing at the early stages of the reaction (section 3.2.1). After 3h of reaction, the liquid produced stabilized at 375 °C or slightly decreased at 350 °C and 390 °C due to the lower amount of solid converted in this time (Figure 3-A and Table S6) and the HDT reactions.

The elemental composition of the HDT liquid product is shown in Figure 4. When compared with the crude oil feedstock (Table 2), the HDT liquid products contained a higher concentration of carbon and hydrogen (Figure 4) even at $t_{reaction}$ = 0 h. Similarly, the concentration of heteroatoms in the liquid product was also significantly smaller at $t_{reaction}$ = 0 h than on the parent crude oil sample, with

deoxygenation, denitrogenation, and desulfurization in the range of 60%, 30% and 50% respectively (Tables S7 to S9). It should be mentioned during heating, H_2 pressure is reduced (10 bar, at room temperature) and that heating up to the reaction temperature takes 20 min. Thus, the significant elimination of heteroatoms during heating suggests these be easily removable under relatively mild conditions or by thermal degradation. Furthermore, HDO, HDS, and, to a lesser extent, HDN (Tables S7 to S9) significantly increased with the reaction time, reaching above 94 %, 96 %, and 78%, respectively, after 3 h of reaction. High denitrogenation levels requires a higher temperature 390 °C, HDN rate was significantly favored at higher temperatures. The efficient removal of heteroatoms suggests that the hetero-compounds in the crude oil feedstock are not in the form of refractory compounds, i.e., polyaromatic sulfur and nitrogen compounds[38], as indicated by Liu et al.[35]. It is relevant to mention that most HTL crude oils from bio-sourced feedstocks, like algae, food waste, and sewage sludge, require two stages of upgrading to remove heteroatoms effectively[23,39,40]. Yet, nearly all lignite crude oil's sulfur, nitrogen, and oxygen were removed after a single hydrotreatment step on NiMoS/P-Al_2O_3 catalyst. Still, in the best-case scenario, 30 ppm of sulfur was found in the liquid, indicating further desulfurization via a second HDT stage, harsher conditions, or blending is necessary to meet the minimum requirements of a drop-in fuel from lignite crude oil.

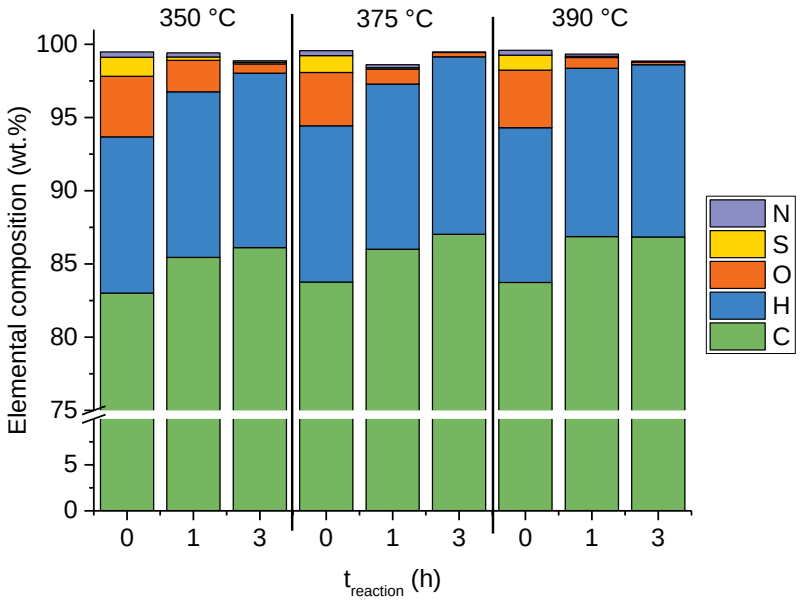

Figure 4. Elemental analysis of the liquid product obtained from HDT of lignite crude oil at different reaction temperatures (350 °C, 375 °C, and 390 °C) and reaction times ($t_{reaction}$).

The evolution of the functional groups upon HDT, determined by ^{13}C NMR, is shown in Figure 5. In comparison with the crude oil, the distribution of the functional groups of the liquid product clearly shows a significant increase in the aliphatic carbon, i.e., from 40.1%, in crude oil, to 54.8 – 74.2% in the liquid, accompanied by a reduction of the aromatic carbon, i.e., 54.3% to 42.3 – 24.0%. When comparing the HDT liquids composition obtained at $t_{reaction}$ = 0 h, it can be observed that the concentration of aromatic C-H and C-C increases with temperature. In contrast, the occurrence of functional groups containing oxygen and aliphatic C follows the opposite trend (Figure 5). The increase of aromatic carbon in the liquid with the reaction temperature for $t_{reaction}$ = 0 h suggests that thermal phenomena cause transformations during reactor heating. Indeed, the UV absorption at λ=290 nm (Figure 6-B), characteristic of polyaromatic compounds, which can be formed by unstable products in the crude oil during heating, clearly increases as a function of temperature for T = 0 h. As the reaction time increases, the concentration of aliphatic C increases together with a reduction of aromatic C as a consequence of hydrogenation, as confirmed by the H/C ratio increase from ≈1.5 at 0 h to >1.6 after 3 h for reaction (Figure 4). Additionally, the $\frac{C_{Aliphatic}}{C_{Aromatic}}$ ratio increases more with the reaction time for higher temperatures due to the faster kinetics of the HDT reactions promoted by the catalyst. While HDT significantly reduced the aromatic C-H bonds concentration, the concentration of aromatic C-C only decreased slightly at 375 °C and 390°C and even increased at 350 °C (Figure 5). Additionally, the $\frac{C-C_{aromatic}}{C_{Aromatic}}.6$ (where 6 refers to the number of carbon atoms in one aromatic ring), which accounts for the average number of C-$C_{Aromatic}$ bonds per aromatic ring, increased from 1.5 at 0 h to 2.0 after 3 h of reaction. It should be mentioned that aromatic C-C bounds can result from polyaromatic hydrocarbons, partially hydrogenated polycyclic-aromatics, like tetraline, and alkylated aromatics, such as toluene. Aromatic ring hydrogenation in polyaromatic compounds decreases for each ring already hydrogenated in the molecule [38,41,42]. Indeed, our previous work screening the upgrading of

various HTL oils has already demonstrated that lignite crude oils were particularly rich in aromatic compounds, which results in a significant concentration of naphthenes and cyclic monoaromatic compounds after HDT[43].

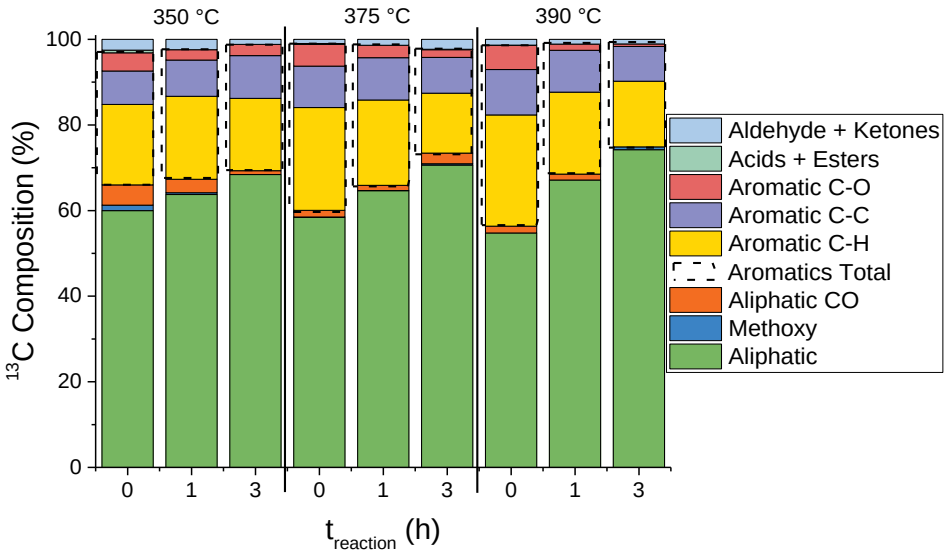

Figure 5. ^{13}C functional group composition of the liquid product obtained from HDT of lignite crude oil at different reaction temperatures (350 °C, 375 °C, and 390 °C) and reaction times ($t_{reaction}$).

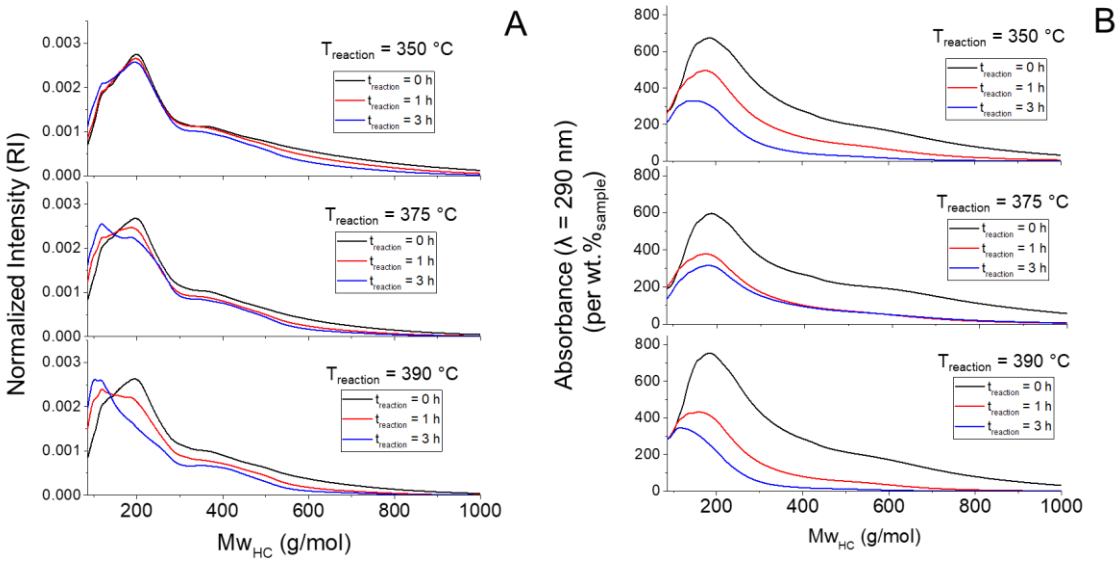

Figure 6. A) Liquid product molecular weight (Mw_{HC}) distribution determined by refraction index (RI), and B) UV absorbance (λ = 290 nm) as a function of the compounds Mw. A hydrocarbon mixture with Mw comprised between 86 g/mol and 1000 g/mol was used as a standard to determine Mw_{HC}.

461

462 The molecular weight (Mw_{HC}) distribution of the HDT liquid products is shown in Figure 6A. At low
463 reaction time, the Mw_{HC} distribution presented a maximum centered at ≈200 g/mol and a maximum
464 molecular weight of 1 000 g/mol. As the reaction time increased, the compounds centered at 200
465 g/mol progressively decreased as a new group of compounds centered at ≈120 g/mol appeared.
466 Similarly, the higher molecular weight compounds progressively disappeared, and at 390 °C after 3 h
467 of reaction, no compounds above 800 g/mol were detected. Indeed, the degree of Mw_{HC} reduction
468 observed in the liquid products after HDT highly depended on the reaction time and temperature,
469 with the average Mw_{HC} (Table S10) ranging from 243 g/mol to 160 g/mol. The average molecular
470 weight of the liquid products is reported in Table S10.
471 The removal of the heteroatom elements, i.e., O, N, and S, is considered to be the main responsible
472 for the significant Mw_{HC} reduction since the cleavage of C-C bonds via hydrogenolysis is not
473 predominant under the reaction conditions used in this study.

474 Figure 6B shows the absorbance at λ=290 nm, characteristic of conjugated polyaromatic compounds,
475 as a function Mw_{HC}. The absorbance decreases as a function of the reaction time due to the full or
476 partial hydrogenation of the polyaromatic compounds. Still, Figure 6B clearly shows that
477 polyaromatics undergo faster conversion in the first hour of a reaction than in the subsequent 2 h, a
478 phenomenon explained by the more straightforward conversion of certain compounds in the oil. Also,
479 at all temperatures, the UV absorption for Mw_{HC} > 300 g/mol decreases fast during HDT, with nealy all
480 polyaromatics in this range being converted at T = 390 °C after 3 h of reaction. However, the refraction
481 index detector (RID – Figure 6A) clearly shows that the amount of compounds with a Mw_{HC} > 300
482 g/mol are only reduced slightly during HDT. The difference between the two detectors suggests that
483 higher Mw_{HC} polyaromatic compounds undergo hydrogenation faster. Indeed, Korre et al. studied the
484 hydrogenation kinetic of multiple polyaromatic compounds identifying that the higher the number of
485 conjugated rings, the faster the hydrogenation reaction rate[44].

The composition of the liquid product, quantified by comprehensive GC×GC/FID (Figure 7), shows a progressive increase in the concentration of aliphatic and mono-aromatic hydrocarbon under harsher reaction conditions, as already suggested by ^{13}C NMR (Figure 5), SEC-DAD (Figure 6B), and elemental analysis (Figure 4) results. At the same time, the oxygenated compounds, such as phenols, ketones, furans, and other high molecular weight compounds, are progressively transformed. Furthermore, the concentration of compounds in the comprehensive GC×GC-FID analysis detection range, i.e., up to ≈C_{40}, progressively increased with HDT reaction time and temperature, which is a consequence of the reduction of the Mw of the samples (Figure 6A). At 390 °C and 3 h of reaction, 88.4 wt.% of the HDT liquid product composition was quantified, with aliphatic and monoaromatic hydrocarbon, mainly composed of naphthenes and partially hydrogenated aromatics, respectively, contributing to ≈75% of the sample. Additionally, 9 wt.% of the liquid was composed of polyaromatic hydrocarbons with two or more aromatic rings. The high concentration of cyclic hydrocarbons in the liquid is a direct consequence of the aromatic nature of the products in the crude oil and, by extension, in lignite. Indeed, in our previous work, we demonstrated that the nature of the feedstock was crucial in determining the composition of the HDT liquid product and that lignite led to an HDT liquid rich in cyclic hydrocarbons[43].

As mentioned before, lignite crude oil was already transformed during the 20 min heating stage of the reactor, as easily observable by the comprehensive GCxGC's significant compound detection boost, i.e., 16.7 wt.% to >56.7 wt.%. While the increase in aromatic content in the liquid showed that thermal phenomena caused at least part of the transformation, the rise in detectable aliphatic and monoaromatic hydrocarbon compounds suggests that catalytic HDT was also responsible for the transformation of the feedstock during the heating stage, indicating that lignite crude oil can undergo significant heteroatoms removal, even under relatively mild conditions.

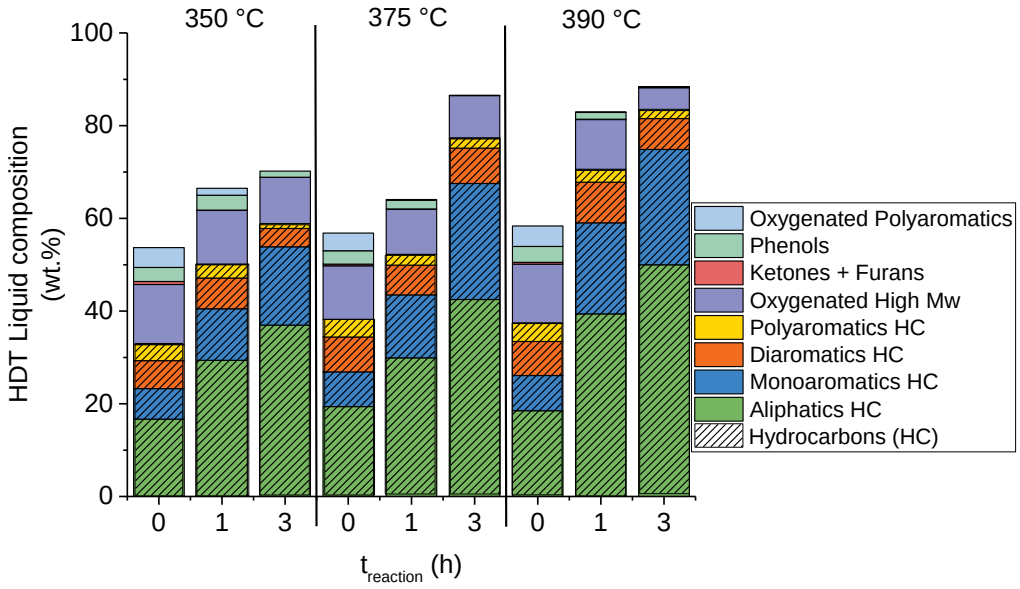

509

510 Figure 7. Composition of HDT liquid as a function of the reaction temperature (350 °C, 375 °C, and 390
511 °C) and reaction time ($t_{reaction}$) detected by GCxGC-TOFMS and quantified by GCxGC-FID

512

513 The distillation curves for the HDT liquid products are shown in Figure 8. As expected SEC results, the
514 number of products in the fuel range increases with the reaction temperature and time. While at 0h,
515 the fuel range products concentration is quite similar at all temperatures (17-20 wt.%), fuel yield
516 quickly rises with the reaction time (Table S11). It is worth mentioning that oxygenated products, like
517 phenols, are present in the fuel product in all cases, except for the experiments performed at 375°C
518 and 390 °C after 3 h of reaction, which are exclusively composed of hydrocarbon molecules.
519 Additionally, diaromatic hydrocarbons are present in all cases and makeup ≈ 5 wt.% of the fuel range
520 products obtained at 375°C and 390 °C after 3 h of reaction. Additionally, the maximum fuel yield
521 obtained at 375°C and 390°C was 47.0 wt.% and 47.6 wt.%, respectively, showing that increasing the
522 HDT temperature has little effect on the overall fuel yield after the elimination of most heteroatoms

(Figure 4). Still, a slight variation in the composition of the fuel range products was observed (Tables S12 and S13), with the test at 375°C yielding more products, i.e., 33.5 wt.% Vs 30..8 wt.%, in the middle distillates range (Bp between 250°C and 350°C) and the test at test at 390°C being more selective for kerosene (Bp between 175°C and 250 °C), i.e., 14.7 wt.% Vs. 11.9 wt.%. The increase in lower Bp products observed at 390 °C might be associated with C-C hydrogenolysis, favored by a higher temperature.

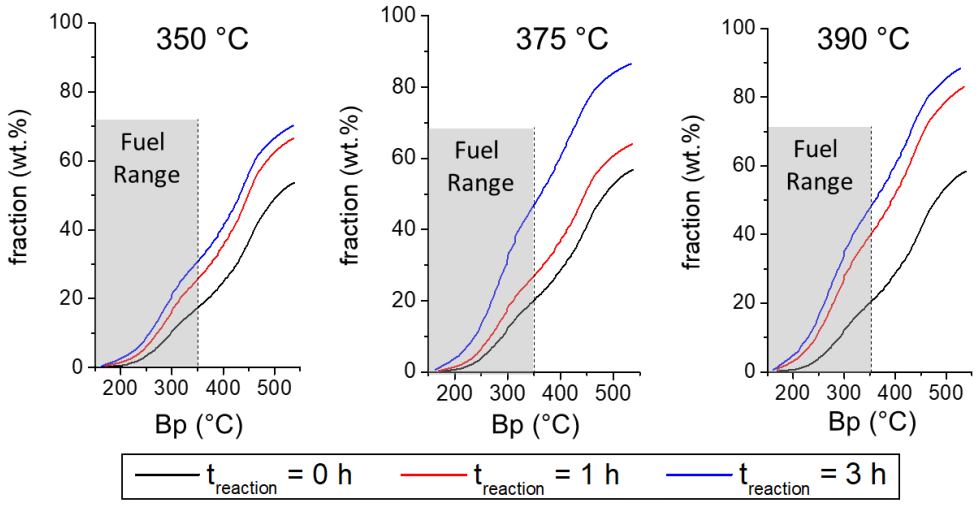

Figure 8. Distillation curve of the hydrotreatment liquid product as a function of reaction time ($t_{reaction}$). Fuel range: Bp < 350°C.

4. CONCLUSION

In several European countries, gross electricity is partly generated by the combustion of lignite. Here, we propose diverting one fraction of the lignite to produce kerosene and diesel through a HTL and single-stage HDT sequence. The overall mass balance of the process, shown in Figure 9, indicates that the HDT liquid yield obtained from lignite under the HTL and HDT conditions used in this study is 8-9 wt.% and 47 wt.% of HDT liquid products have a boiling point in the range of standard fuels, i.e., Bp < 350°C (Figure 8). The unsatisfactory production of crude oil during HTL, i.e., 12.3%, is responsible for the low overall conversion of lignite into fuel. Indeed, the HDT liquid yield obtained in this study, i.e.,

65-73 wt.%, was comparable to that in the literature when upgrading HTL biocrudes produced from different feedstocks[45–49]. The low crude oil yield can be explained by the experimental conditions used in the HTL process, as Liu et al. were able to increase the crude oil production to 34 wt.% by using a lower HTL reaction time (5 min) and higher temperature (440 °C). Additionally, the use of catalysts[50] and recycling the aqueous phase[51] are known to increase crude yield during HTL. Therefore, adequate process optimization can orient a more significant fraction of lignite towards fuel generation.

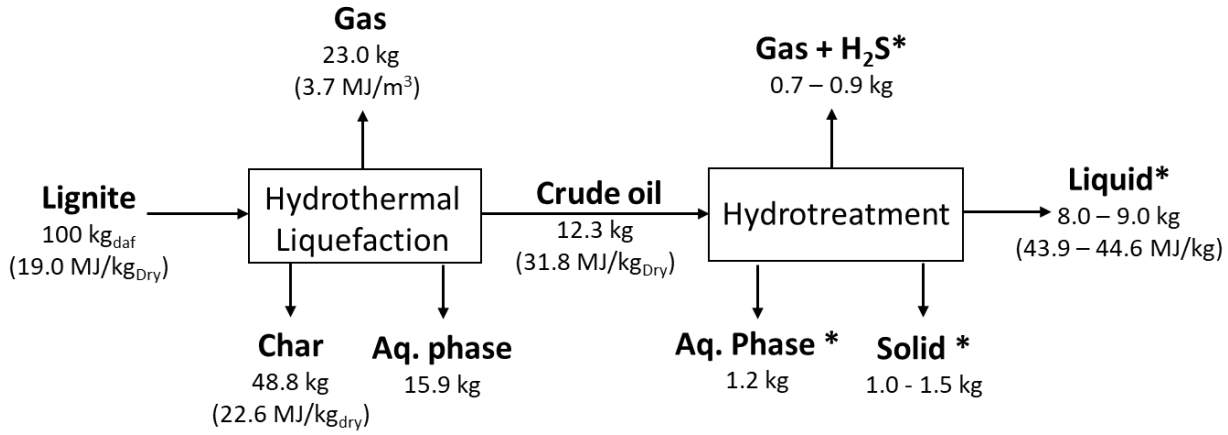

Figure 9. Block flow diagram of the transformation of lignite through hydrothermal liquefaction (HDT) and subsequent hydrotreatment of the HTL crude oil. Mass basis = 100 kg of dry ash-free lignite (kg_{daf}). The values in brackets refer to the calorific value of the respective streams and were determined by using the expression from [52]. *values determined using the data from HDT performed during 3 h at temperatures of 375°C and 390°C (Figures 3-A and 4).

The hydrotreatment experiments showed lignite's crude oil to be quite easily hydrotreated. Near complete heteroatom removal was attained with a single HDT stage and using a milder pseudo-WHSV (equation 5) than those reported in the literature for pilot-scale bio-based crude oil HDT[47,53]. After HDT, despite a significant improvement in fuel quality, i.e., heteroatom removal and hydrogenation, substantial amounts of aromatic compounds, particularly monoaromatic and diaromatic compounds (≈45% of fuel range products), are still present in all products. This suggests that further upgrading or

harsher conditions, i.e., higher contact time and H_2 pressure, are required. Indeed, aromatics have low cetane numbers, which can be detrimental for using the middle distillate in diesel fuels[54]. In addition to decreasing the aromatic content in the liquid product, our results showed that harshening HDT conditions did not significantly augment the fuel range products, suggesting that subsequent hydrocracking or using an HDT catalyst with acid properties might be necessary. Nevertheless, the crude oil obtained from the hydrothermal liquefaction of lignite has an excellent potential for producing hydrocarbon fuels, particularly when compared with other feedstocks typically used in the HTL process, like sewage sludge and algae[39,55]. Finally, it is important to mention that the presence of this aromatic fraction can be a benefit, acting as a polar solvent in the case of co-processing between HTL of lignite and less proper biogenic feedstocks, such as biomass or sewage sludge.

While lignite is not a green feedstock, its easily upgradable products obtained during HTL can be beneficial under mixed hydrothermal liquefaction with greener feedstocks, like lignocellulosic biomass, sewage sludge or algae, which yield crude oils more difficult to upgrade as proposed, for instance, by Wang et al. [56]. Indeed, it was shown that the hydrothermal liquefaction of a mixture of Jingou lignite, wheat straw, and plastic waste could provide a synergetic effect on oil yields. Synergetic effects were also observed in the co-liquefaction of coal and polymers (polypropylene and polystyrene) by Y. Shen et al.[57]. Finally, it is worth mentioning that the char from lignite HTL can be further used for electricity production, the original purpose of lignite.

5. Acknowledgements

The authors gratefully acknowledge the financial support of the European Commission Research Programme of the Research Fund for Coal and Steel for the project HyCon (Grant agreement: 899471). In the case of Polish authors, this scientific work is published as part of an international project co-financed by the program of the Ministry of Science and Higher Education entitled "PMW" in the years 2020 -2023 agreement No. 5157/FBWiS/2020/2021/2

6. References

(1) Tollefson, J. What the War in Ukraine Means for Energy, Climate and Food. *Nature 604*, 232–233.

(2) *Renewables 2019*; IEA: Paris, 2019. https://www.iea.org/reports/renewables-2019.

(3) Lignite Energy Council. *Uses and Benefits of Lignite*.

(4) Eurostat. *Eurostat*. ec.europa.eu/eurostat.

(5) Kershaw, J. R. Extraction of Victorian Brown Coals with Supercritical Water. *Fuel Processing Technology* **1986**, *13* (2), 111–124. https://doi.org/10.1016/0378-3820(86)90053-6.

(6) Deshpande, G. V.; Holder, G. D.; Bishop, A. A.; Gopal, J.; Wender, I. Extraction of Coal Using Supercritical Water. *Fuel* **1984**, *63* (7), 956–960. https://doi.org/10.1016/0016-2361(84)90318-1.

(7) Hu, H.; Guo, S.; Hedden, K. Extraction of Lignite with Water in Sub- and Supercritical States. *Fuel Processing Technology* **1998**, *53* (3), 269–277. https://doi.org/10.1016/S0378-3820(97)00057-X.

(8) Nikolopoulos, N.; Violidakis, I.; Karampinis, E.; Agraniotis, M.; Bergins, C.; Grammelis, P.; Kakaras, E. Report on Comparison among Current Industrial Scale Lignite Drying Technologies (A Critical Review of Current Technologies). *Fuel* **2015**, *155*, 86–114. https://doi.org/10.1016/j.fuel.2015.03.065.

(9) Hartman, B. E.; Hatcher, P. G. Valuable Crude Oil from Hydrothermal Liquefaction of an Aliphatic Coal. *Energy Fuels* **2014**, *28* (12), 7538–7551. https://doi.org/10.1021/ef5018708.

(10) Liu, P.; Wang, L.; Zhou, Y.; Pan, T.; Lu, X.; Zhang, D. Effect of Hydrothermal Treatment on the Structure and Pyrolysis Product Distribution of Xiaolongtan Lignite. *Fuel* **2016**, *164*, 110–118. https://doi.org/10.1016/j.fuel.2015.09.092.

(11) Li, H.; Wu, S.; Wu, Y.; Wang, H.; Zhang, Z.; Huang, S.; Gao, J. Effects of Hydrothermal Treatment on Physico-Chemcial Structures and Liquefaction Behaviors of Lignite. *Fuel* **2020**, *263*, 116636. https://doi.org/10.1016/j.fuel.2019.116636.

(12) Lelevic, A.; Souchon, V.; Geantet, C.; Lorentz, C.; Moreaud, M. Advanced Data Preprocessing for Comprehensive Two-Dimensional Gas Chromatography with Vacuum Ultraviolet Spectroscopy Detection. *Journal of Separation Science* **2021**, *44* (22), 4141–4150. https://doi.org/10.1002/jssc.202100528.

(13) Scanlon, J. T.; Willis, D. E. Calculation of Flame Ionization Detector Relative Response Factors Using the Effective Carbon Number Concept. *Journal of Chromatographic Science* **1985**, *23* (8), 333–340. https://doi.org/10.1093/chromsci/23.8.333.

(14) Liu, P.; Zhang, D. Effect of Hydrothermal Treatment on the Carbon Structure of Inner Mongolia Lignite. *International Journal of Coal Science & Technology* **2020**, *7* (3), 493–503. https://doi.org/10.1007/s40789-020-00356-7.

(15) Shi, Z.; Jin, L.; Zhou, Y.; Li, Y.; Hu, H. Effect of Hydrothermal Treatment on Structure and Liquefaction Behavior of Baiyinhua Coal. *Fuel Processing Technology* **2017**, *167*, 648–654. https://doi.org/10.1016/j.fuproc.2017.08.015.

(16) Maes, I. I.; Gryglewicz, G.; Machnikowska, H.; Yperman, J.; Franco, D. V.; Mullens, J.; Van Poucke, L. C. Rank Dependence of Organic Sulfur Functionalities in Coal. *Fuel* **1997**, *76* (5), 391–396. https://doi.org/10.1016/S0016-2361(97)85515-9.

(17) Patwardhan, P. R.; Timko, M. T.; Class, C. A.; Bonomi, R. E.; Kida, Y.; Hernandez, H. H.; Tester, J. W.; Green, W. H. Supercritical Water Desulfurization of Organic Sulfides Is Consistent with Free-Radical Kinetics. *Energy Fuels* **2013**, *27* (10), 6108–6117. https://doi.org/10.1021/ef401150w.

(18) Meng, N.; Jiang, D.; Liu, Y.; Gao, Z.; Cao, Y.; Zhang, J.; Gu, J.; Han, Y. Sulfur Transformation in Coal during Supercritical Water Gasification. *Fuel* **2016**, *186*, 394–404. https://doi.org/10.1016/j.fuel.2016.08.097.

(19) Liao, J.; Fei, Y.; Marshall, M.; Chaffee, A. L.; Chang, L. Hydrothermal Dewatering of a Chinese Lignite and Properties of the Solid Products. *Fuel* **2016**, *180*, 473–480. https://doi.org/10.1016/j.fuel.2016.04.027.
(20) Liu, shucheng; Zhao, H.; Fan, T.; Zhou, J.; Liu, X.; Li, Y.; Zhao, G.; Wang, Y.; Zeng, M. Investigation on Chemical Structure and Hydrocarbon Generation Potential of Lignite in the Different Pretreatment Process. *Fuel* **2021**, *291*, 120205. https://doi.org/10.1016/j.fuel.2021.120205.
(21) Liu, C.; Li, J.; Lin, Y. Optimization Study of Sub/Supercritical Water Liquefication of Lignite: Fast Liquefaction for High Bio-Oil Yield. *International Journal of Hydrogen Energy* **2019**, *44* (39), 21406–21412. https://doi.org/10.1016/j.ijhydene.2019.06.140.
(22) Calkins, W. H. The Chemical Forms of Sulfur in Coal: A Review. *Fuel* **1994**, *73* (4), 475–484. https://doi.org/10.1016/0016-2361(94)90028-0.
(23) Fraga, G.; Batalha, N.; Kumar, A.; Bhaskar, T.; Konarova, M.; Perkins, G. Chapter 5 - Advances in Liquefaction for the Production of Hydrocarbon Biofuels. In *Hydrocarbon Biorefinery*; Maity, S. K., Gayen, K., Bhowmick, T. K., Eds.; Elsevier, 2022; pp 127–176. https://doi.org/10.1016/B978-0-12-823306-1.00009-1.
(24) Yan, S.; Xia, D.; Liu, X. Beneficial Migration of Sulfur Element during Scrap Tire Depolymerization with Supercritical Water: A Molecular Dynamics and DFT Study. *Science of The Total Environment* **2021**, *776*, 145835. https://doi.org/10.1016/j.scitotenv.2021.145835.
(25) Audu, M.; Wang, H.; Arellano, D.; Cheng, F.; Dehghanizadeh, M.; Jarvis, J. M.; Yan, J.; Brewer, C. E.; Jena, U. Ash-Pretreatment and Hydrothermal Liquefaction of Filamentous Algae Grown on Dairy Wastewater. *Algal Research* **2021**, *57*, 102282. https://doi.org/10.1016/j.algal.2021.102282.
(26) Chen, W.-T.; Qian, W.; Zhang, Y.; Mazur, Z.; Kuo, C.-T.; Scheppe, K.; Schideman, L. C.; Sharma, B. K. Effect of Ash on Hydrothermal Liquefaction of High-Ash Content Algal Biomass. *Algal Research* **2017**, *25*, 297–306. https://doi.org/10.1016/j.algal.2017.05.010.
(27) Liu, H.; Chen, Y.; Yang, H.; Gentili, F. G.; Söderlind, U.; Wang, X.; Zhang, W.; Chen, H. Conversion of High-Ash Microalgae through Hydrothermal Liquefaction. *Sustainable Energy Fuels* **2020**, *4* (6), 2782–2791. https://doi.org/10.1039/C9SE01114E.
(28) Liu, R.; Tian, W.; Kong, S.; Meng, Y.; Wang, H.; Zhang, J. Effects of Inorganic and Organic Acid Pretreatments on the Hydrothermal Liquefaction of Municipal Secondary Sludge. *Energy Conversion and Management* **2018**, *174*, 661–667. https://doi.org/10.1016/j.enconman.2018.08.058.
(29) Shafizadeh, A.; Shahbeig, H.; Nadian, M. H.; Mobli, H.; Dowlati, M.; Gupta, V. K.; Peng, W.; Lam, S. S.; Tabatabaei, M.; Aghbashlo, M. Machine Learning Predicts and Optimizes Hydrothermal Liquefaction of Biomass. *Chemical Engineering Journal* **2022**, *445*, 136579. https://doi.org/10.1016/j.cej.2022.136579.
(30) Oner, M.; Oner, G.; Bolat, E.; Yalin, G.; Kavlak, C.; Dincer, S. The Effect of Ash and Ash Constituents on the Liquefaction Yield of Turkish Lignites and Asphaltites. *Fuel* **1994**, *73* (10), 1658–1666. https://doi.org/10.1016/0016-2361(94)90147-3.
(31) Prado, G. H. C.; Rao, Y.; de Klerk, A. Nitrogen Removal from Oil: A Review. *Energy Fuels* **2017**, *31* (1), 14–36. https://doi.org/10.1021/acs.energyfuels.6b02779.
(32) ASTM D7566-22 -Standard Specification for Aviation Turbine Fuel Containing Synthesized Hydrocarbons. In *ASTM Volume 05.04: Petroleum Products, Liquid Fuels, And Lubricants (IV): D7412 – D8128*; ASTM, 2023; Vol. 05.04, p 2074.
(33) Prado, G. H. C.; Rao, Y.; de Klerk, A. Nitrogen Removal from Oil: A Review. *Energy Fuels* **2017**, *31* (1), 14–36. https://doi.org/10.1021/acs.energyfuels.6b02779.
(34) Stefanova, M.; Marinov, S. P.; Magnier, C. Aliphatic Biomarkers from Miocene Lignites Desulphurization. *Fuel* **1999**, *78* (12), 1395–1406. https://doi.org/10.1016/S0016-2361(99)00068-X.

(35) Liu, J.; Wei, X.-Y.; Zhang, D.-D.; Li, Z.-K.; Lv, J.-H.; Wang, T.-M.; Gui, J.; Qu, M.; Guo, L.-L.; Zong, Z.-M.; Li, W.; Kong, L.-X. Characterization of Heteroatom-Containing Species in the Soluble Portion from the Ethanolysis of the Extraction Residue from Xinghe Lignite by Electrospray Ionization Fourier Transform Ion Cyclotron Resonance Mass Spectrometry. *Fuel* **2016**, *173*, 222–229. https://doi.org/10.1016/j.fuel.2016.01.059.
(36) Saturnino, D. Compréhension de la relation entre la structure physico-chimique et l'activité des catalyseurs d'HDS vieillis, Université de Lyon, 2014.
(37) Zhu, C.; Gutiérrez, O. Y.; Santosa, D. M.; Kutnyakov, I.; Weindl, R.; Shi, H.; Wang, H. Impact of Coprocessing Biocrude with Petroleum Stream on Hydrotreating Catalyst Stability. *Energy Fuels* **2022**, *36* (16), 9133–9146. https://doi.org/10.1021/acs.energyfuels.2c01748.
(38) Girgis, M. J.; Gates, B. C. Reactivities, Reaction Networks, and Kinetics in High-Pressure Catalytic Hydroprocessing. *Ind. Eng. Chem. Res.* **1991**, *30* (9), 2021–2058. https://doi.org/10.1021/ie00057a001.
(39) Cronin, D. J.; Subramaniam, S.; Brady, C.; Cooper, A.; Yang, Z.; Heyne, J.; Drennan, C.; Ramasamy, K. K.; Thorson, M. R. Sustainable Aviation Fuel from Hydrothermal Liquefaction of Wet Wastes. *Energies* **2022**, *15* (4). https://doi.org/10.3390/en15041306.
(40) Xu, D.; Lin, G.; Guo, S.; Wang, S.; Guo, Y.; Jing, Z. Catalytic Hydrothermal Liquefaction of Algae and Upgrading of Biocrude: A Critical Review. *Renewable and Sustainable Energy Reviews* **2018**, *97*, 103–118. https://doi.org/10.1016/j.rser.2018.08.042.
(41) Cooper, B. H.; Donnis, B. B. L. Aromatic Saturation of Distillates: An Overview. *Applied Catalysis A: General* **1996**, *137* (2), 203–223. https://doi.org/10.1016/0926-860X(95)00258-8.
(42) Stanislaus, A.; Cooper, B. H. Aromatic Hydrogenation Catalysis: A Review. *Catalysis Reviews* **1994**, *36* (1), 75–123. https://doi.org/10.1080/01614949408013921.
(43) Batalha, N.; Checa, R.; Lorentz, C.; Afanasiev, P.; Stańczyk, K.; Kapusta, K.; Laurenti, D.; Geantet, C. Lignite and Biomass Waste Hydrothermal Liquefaction Crude Upgrading by Hydrotreatment. *Energy Fuels* **2023**, *37* (14), 10506–10520. https://doi.org/10.1021/acs.energyfuels.3c01550.
(44) Korre, S. C.; Klein, M. T.; Quann, R. J. Polynuclear Aromatic Hydrocarbons Hydrogenation. 1. Experimental Reaction Pathways and Kinetics. *Ind. Eng. Chem. Res.* **1995**, *34* (1), 101–117. https://doi.org/10.1021/ie00040a008.
(45) Castello, D.; Haider, M. S.; Rosendahl, L. A. Catalytic Upgrading of Hydrothermal Liquefaction Biocrudes: Different Challenges for Different Feedstocks. *Renewable Energy* **2019**, *141*, 420–430. https://doi.org/10.1016/j.renene.2019.04.003.
(46) Sharma, K.; Castello, D.; Haider, M. S.; Pedersen, T. H.; Rosendahl, L. A. Continuous Co-Processing of HTL Bio-Oil with Renewable Feed for Drop-in Biofuels Production for Sustainable Refinery Processes. *Fuel* **2021**, *306*, 121579. https://doi.org/10.1016/j.fuel.2021.121579.
(47) Subramaniam, S.; Santosa, D. M.; Brady, C.; Swita, M.; Ramasamy, K. K.; Thorson, M. R. Extended Catalyst Lifetime Testing for HTL Biocrude Hydrotreating to Produce Fuel Blendstocks from Wet Wastes. *ACS Sustainable Chem. Eng.* **2021**, *9* (38), 12825–12832. https://doi.org/10.1021/acssuschemeng.1c02743.
(48) da Costa Magalhães, B.; Checa, R.; Lorentz, C.; Afanasiev, P.; Laurenti, D.; Geantet, C. Catalytic Hydroconversion of HTL Micro-Algal Bio-Oil into Biofuel over NiWS/Al2O3. *Algal Research* **2023**, *71*, 103012. https://doi.org/10.1016/j.algal.2023.103012.
(49) Magalhães, B. C.; Checa, R.; Lorentz, C.; Prévot, M.; Afanasiev, P.; Laurenti, D.; Geantet, C. Catalytic Hydrotreatment of Algal HTL Bio-Oil over Phosphide, Nitride, and Sulfide Catalysts. *ChemCatChem* **2023**, *15* (9), e202300025. https://doi.org/10.1002/cctc.202300025.
(50) Nagappan, S.; Bhosale, R. R.; Nguyen, D. D.; Chi, N. T. L.; Ponnusamy, V. K.; Woong, C. S.; Kumar, G. Catalytic Hydrothermal Liquefaction of Biomass into Bio-Oils and Other Value-Added Products – A Review. *Fuel* **2021**, *285*, 119053. https://doi.org/10.1016/j.fuel.2020.119053.
(51) Watson, J.; Wang, T.; Si, B.; Chen, W.-T.; Aierzhati, A.; Zhang, Y. Valorization of Hydrothermal Liquefaction Aqueous Phase: Pathways towards Commercial Viability. *Progress in Energy and Combustion Science* **2020**, *77*, 100819. https://doi.org/10.1016/j.pecs.2019.100819.

(52) Channiwala, S. A.; Parikh, P. P. A Unified Correlation for Estimating HHV of Solid, Liquid and Gaseous Fuels. *Fuel* **2002**, *81* (8), 1051–1063. https://doi.org/10.1016/S0016-2361(01)00131-4.
(53) Verdier, S.; Mante, O. D.; Hansen, A. B.; Poulsen, K. G.; Christensen, J. H.; Ammtizboll, N.; Gabrielsen, J.; Dayton, D. C. Pilot-Scale Hydrotreating of Catalytic Fast Pyrolysis Biocrudes: Process Performance and Product Analysis. *Sustainable Energy Fuels* **2021**, *5* (18), 4668–4679. https://doi.org/10.1039/D1SE00540E.
(54) Song, C.; Ma, X. New Design Approaches to Ultra-Clean Diesel Fuels by Deep Desulfurization and Deep Dearomatization. *Applied Catalysis B: Environmental* **2003**, *41* (1), 207–238. https://doi.org/10.1016/S0926-3373(02)00212-6.
(55) Hao, B.; Xu, D.; Jiang, G.; Sabri, T. A.; Jing, Z.; Guo, Y. Chemical Reactions in the Hydrothermal Liquefaction of Biomass and in the Catalytic Hydrogenation Upgrading of Biocrude. *Green Chem.* **2021**, *23* (4), 1562–1583. https://doi.org/10.1039/D0GC02893B.
(56) Wang, B.; Huang, Y.; Zhang, J. Hydrothermal Liquefaction of Lignite, Wheat Straw and Plastic Waste in Sub-Critical Water for Oil: Product Distribution. *Journal of Analytical and Applied Pyrolysis* **2014**, *110*, 382–389. https://doi.org/10.1016/j.jaap.2014.10.004.
(57) Shen, Y.; Wu, H.; Pan, Z. Co-Liquefaction of Coal and Polypropylene or Polystyrene in Hot Compressed Water at 360–430°C. *Fuel Processing Technology* **2012**, *104*, 281–286. https://doi.org/10.1016/j.fuproc.2012.05.023.